



Unipolar vertical transport in GaN/AlGaN/GaN heterostructures

D. N. Nath, Z. C. Yang, C.-Y. Lee, P. S. Park, Y.-R. Wu, and S. Rajan

Citation: [Applied Physics Letters](#) **103**, 022102 (2013); doi: 10.1063/1.4813309

View online: <http://dx.doi.org/10.1063/1.4813309>

View Table of Contents: <http://scitation.aip.org/content/aip/journal/apl/103/2?ver=pdfcov>

Published by the [AIP Publishing](#)



Re-register for Table of Content Alerts

Create a profile.



Sign up today!



Unipolar vertical transport in GaN/AlGaN/GaN heterostructures

D. N. Nath,¹ Z. C. Yang,¹ C.-Y. Lee,² P. S. Park,¹ Y.-R. Wu,² and S. Rajan¹

¹Department of Electrical and Computer Engineering, The Ohio State University, Columbus, Ohio 43210, USA

²Institute of Photonics and Optoelectronics and Department of Electrical Engineering, National Taiwan University, Taipei 10617, Taiwan

(Received 8 May 2013; accepted 19 June 2013; published online 8 July 2013)

In this letter, we report on unipolar vertical transport characteristics in c-plane GaN/AlGaN/GaN heterostructures. Vertical current in heterostructures with random alloy barriers was found to be independent of dislocation density and heterostructure barrier height. Percolation-based transport due to random alloy fluctuations in the ternary AlGaN is suggested as the dominant transport mechanism. This hypothesis is supported by simulations using drift-diffusion transport model incorporating statistical fluctuations of Al-composition and confirmed through experiments showing that non-random or digital AlGaN alloys and polarization-engineered binary GaN barriers can eliminate percolation transport and reduce leakage significantly. The understanding of vertical transport and methods for effective control proposed here will greatly impact III-nitride unipolar vertical devices. © 2013 AIP Publishing LLC. [<http://dx.doi.org/10.1063/1.4813309>]

Recently, there has been renewed interest in unipolar III-nitride vertical devices such as resonant tunneling diodes (RTD),^{1–3} hot electron transistors (HET),^{4,5} and tunnel-injection hot electron transfer amplifiers (THETA).^{6–8} III-nitride vertical transistors, in particular, are of interest since heterojunction bipolar transistors, which have achieved maturity in the InP/GaAs material system, are not viable due to the low hole mobility and lifetime in GaN. However, high vertical leakage currents in n-GaN/AlGaN/n-GaN heterostructures have held back the development of unipolar vertical III-nitride transistors. In this letter, we propose that percolation based leakage due to alloy fluctuations in the ternary AlGaN barrier dominates vertical transport, which is supported by simulations performed using drift-diffusion model of transport incorporating such statistical fluctuations in Al-compositions. We also show that eliminating the random alloy barriers can provide control of vertical transport. The results presented here are expected to have important impact on a range of III-nitride devices such as HEMTs and light emitting diodes (LEDs), as well as vertical transport devices such as current aperture vertical electron transfer (CAVET)^{9,10} transistors, RTD, and hot electron transistors.

To study unipolar transport characteristic in III-nitride heterostructures, we investigate an epitaxial stack as shown in Figure 1(a), which consists of a 15–20 nm of degenerately doped n⁺-GaN top contact layer and an Al_xGa_{1-x}N barrier 30–35 nm thick. The n⁺-GaN template on which samples are grown serves as the bottom n-contact. The epitaxial stacks for the devices were grown by plasma-assisted molecular beam epitaxy (MBE) using a Veeco 930 system equipped with a uni-bulb Veeco N₂ plasma source. Commercially available Ga-polar free-standing n-doped GaN substrates (threading dislocation density (TDD) $\sim 5 \times 10^7 \text{ cm}^{-2}$) from St. Gobain were used for the growths. High-resolution X-ray diffractometer scans were done to verify the thicknesses and compositions of epitaxial layers. Al (20 nm)/Ni (20 nm)/Au (100 nm)/Ni (20 nm) were e-beam evaporated for top-contact metal stack. An inductively coupled plasma/re-active ion (ICP-RIE) etch recipe using

40 V RIE and 40 W ICP power with 50 sccm Cl₂/5 sccm BCl₃ was used to achieve a mesa isolation with a controlled etch rate. Depending on the device, mesa area was between 90 and 120 μm^2 . Devices were probed using sub-micron probe tips and measured using an Agilent B1500 Semiconductor Parameter Analyzer.

To investigate the effect of heterostructure barrier height on reverse bias leakage, a series of three samples with Al-composition 16%, 27%, and 37% in the AlGaN barrier were grown, with thickness fixed at 30 nm. As seen in the energy band diagrams (Figure 1(b)) obtained using self-consistent 1-D Schrodinger-Poisson simulator BANDENG,¹¹ AlGaN barrier with 16% Al-composition provides a heterojunction barrier in excess of 0.5 eV from the base Fermi level at equilibrium. The reverse bias leakage current due to Fowler-Nordheim tunneling associated with such a heterostructure with 16% Al-composition was estimated theoretically using analytical calculations, and using Atlas Silvaco¹¹ modeling. As seen in Figure 1(c), theoretically, negligible leakage is expected up to reverse bias of 3 V. However, the typical current densities measured experimentally on devices fabricated were found to be orders of magnitude higher. Figure 1(c) also shows the measured vertical I–V characteristics of the samples with 27% and 37% Al-compositions in the barrier. The magnitude of leakage current in reverse bias was similar for these three samples despite a significant difference in their heterostructure barrier heights. While both thermionic and tunnel current would theoretically be expected to vary by orders of magnitude with such changes in the barrier height, our experiments show that the AlGaN composition had negligible effect on the vertical current leakage in GaN/AlGaN/GaN heterostructures. We can therefore discount tunneling or thermionic emission mechanisms. Temperature dependence of the IV characteristics (Figure 1(d)) revealed that vertical conductivity did not vary significantly with temperature. We conclude that the origin of leakage in heterostructures is not a thermally activated mechanism such as trap-assisted tunneling¹² or thermionic emission over the barrier.

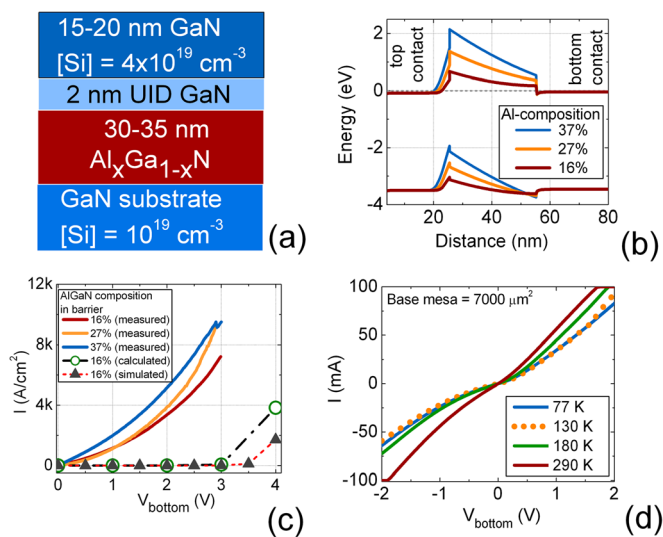


FIG. 1. Effect of heterojunction barrier height on leakage (a) typical epitaxial stack of devices used in this study. (b) Energy band diagrams of device structures with $\text{Al}_x\text{Ga}_{1-x}\text{N}$ barrier with $x=0.16, 0.27,$ and 0.37 . (c) Calculated, simulated and experimentally measured vertical leakage current densities corresponding to an $\text{Al}_{0.16}\text{Ga}_{0.84}\text{N}$ barrier compared to measured leakage for AlGaIn barrier with 25% and 37% Al-composition. (d) Temperature-dependent vertical leakage current showing weak temperature dependence.

TDD, particularly related to screw type dislocations, is widely believed to impact^{13,14} reverse bias leakage in AlGaIn/GaN Schottky diodes and HEMTs.¹⁵ TDDs are also found to affect vertical reverse bias leakage in bipolar heterostructures such as LEDs.^{16,17} However, the impact of TDDs on unipolar semiconductor heterojunction leakage has not been investigated. It should be noted that unlike in metal/semiconductor and bipolar structures where reverse bias leakage is significantly small in magnitude ($\ll 1 \text{ A/cm}^2$ at a few volts), unipolar $n\text{-GaN}/\text{AlGaIn}/n\text{-GaN}$ heterostructures exhibit much higher vertical leakage current (\sim a few kA/cm^2 at 1 V bias). To investigate the effect of dislocations, epitaxial structures were grown on a low-dislocation density bulk GaN substrate¹¹ (sample LD, TDD $< 10^5 \text{ cm}^{-2}$) and a higher dislocation density HVPE grown substrate¹¹ (sample HD, TDD $\sim 5 \times 10^7 \text{ cm}^{-2}$). Both samples were grown and processed together to eliminate growth and process variations. Atomic Force Microscope (AFM) scans (figures in supplementary material¹¹) of surface morphologies of the epitaxial stack for sample HD showed ~ 30 black pits corresponding to screw-type TDDs in a $5 \mu\text{m} \times 5 \mu\text{m}$ scan area indicating TDD $\sim 10^8 \text{ cm}^{-2}$, while no such pits were observed in the AFM scan for sample LD indicating TDD $< 10^5 \text{ cm}^{-2}$. I-V characteristics for $\text{GaN}/\text{AlGaIn}/\text{GaN}$ structures (figure in supplementary material¹¹) revealed that despite three orders of magnitude difference in TDDs, the vertical currents observed in samples LD and HD were very similar. This shows that TDDs are not the primary factor responsible for the anomalous high currents in unipolar $\text{GaN}/\text{AlGaIn}/\text{GaN}$ heterostructures.

Since neither heterojunction barrier height nor a reduction in TDDs affect the behavior of $\text{GaN}/\text{AlGaIn}/\text{GaN}$ heterostructures, and since there is almost no temperature dependence in the current density, our observations suggest that electrons see almost zero effective barrier to transport

across the heterojunction. We propose that percolation-based transport through the Ga-rich regions of AlGaIn is the dominant current mechanism in all the samples described earlier. Such percolation-based transport can be attributed to composition fluctuations in ternary alloy layer¹⁸ due to statistical distribution of Ga and Al atoms in group-III sites. To model this, a 2D finite element Poisson and drift-diffusion solver^{18,19} was applied to study the percolation-based transport behavior. The fluctuations in Al and Ga compositions (Fig. 2(a)) were generated by using a random number generator. The average Al composition of the layer was kept at 20% as the fluctuations in Al-compositions were generated. In every run, the program generated different Al distributions since it was fully randomized. They all showed similar trend. Therefore, we chose one of the results and presented here. The polarization charges, bandgap, effective mass at different locations are changed with the Al composition. A very small mesh size is applied to including this nanoscale fluctuation. After incorporating the statistical fluctuation of Al-composition in the AlGaIn layer, the vertical current estimated from this simulation was found to be more than 5 orders of magnitude higher than that estimated without incorporating fluctuations in the layer (Figure 2(b)), which indicated that percolation-based transport was most likely responsible for the observed leakage in unipolar $\text{GaN}/\text{AlGaIn}/\text{GaN}$ samples. The Al fluctuation would also enhance the tunneling process, where the calculated current might be even closer to the experimental result. This will be our future work.

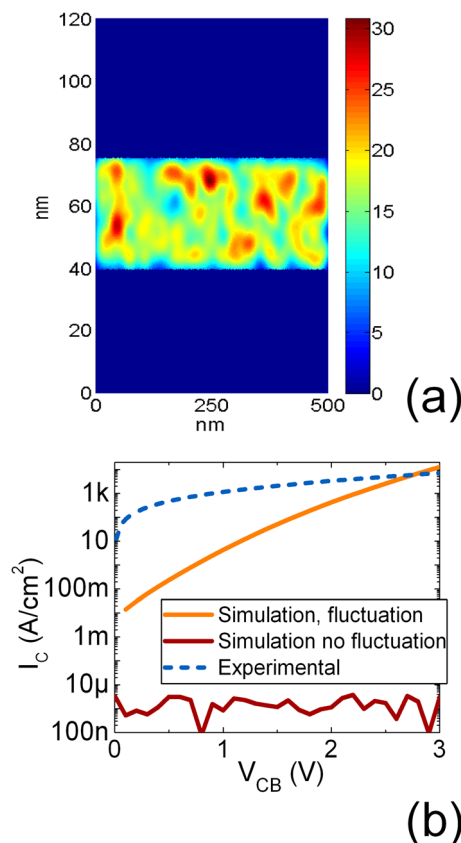


FIG. 2. (a) Modeling of statistical fluctuations of Al-composition in ternary $\text{Al}_{0.20}\text{Ga}_{0.80}\text{N}$ layer. (b) Comparison of measured leakage current densities with those estimated from 2D FEM drift-diffusion transport with and without incorporating statistical fluctuations of Al-composition.

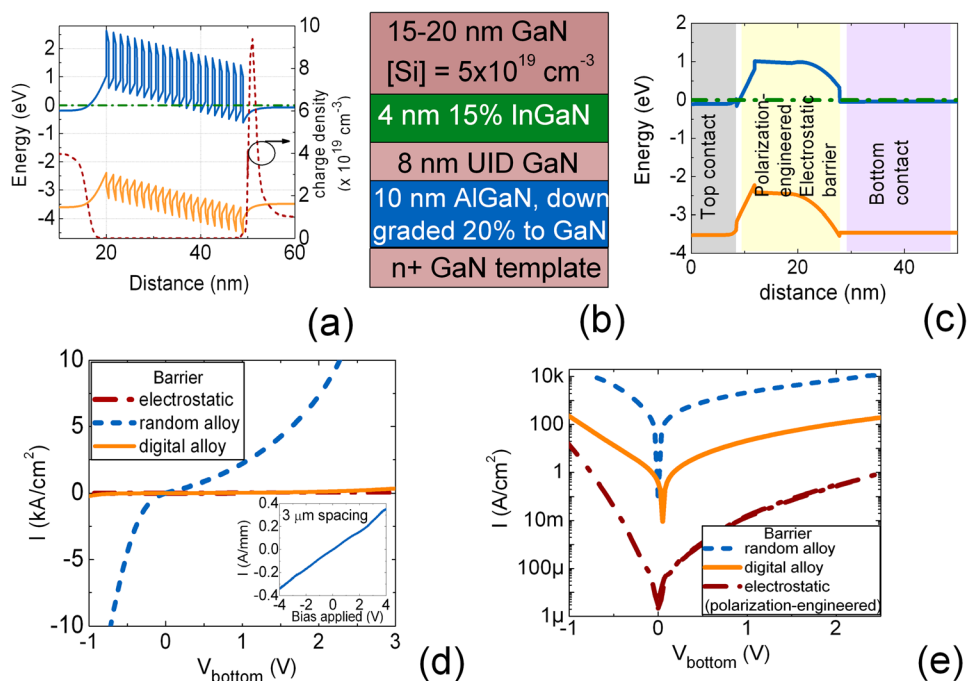


FIG. 3. (a) Energy band diagram of the sample D1 with a digital AlGaIn barrier. (b) Epitaxial stack of the sample with polarization-engineered binary GaN barrier. (c) Energy band diagram of the same. Comparison of measured leakage for samples with random alloy, binary GaN, and digital alloys as barriers in (d) linear (e) log scale. Inset to Figure 3(d) shows the lateral I-V between two top-contacts of the same device indicating its linear and Ohmic nature (the digital alloy sample).

To directly test the percolation-based transport hypothesis, two separate barrier configurations were explored that both eliminate random alloy fluctuations and were compared with random $\text{Al}_{0.3}\text{Ga}_{0.7}\text{N}$ barriers (sample R). The first approach used was a digital AlGaIn barrier (sample D) with alloy barrier grown by repetition of 2 ML AlN/4 ML GaN digital periods. Such an approach eliminates the possibility of statistical fluctuations that could lead to Ga-rich regions in the AlGaIn. The number of digital periods was such that the barrier corresponded to 25–30 nm of AlGaIn with average composition 25% verified by dynamic XRD simulations. Figure 3(a) shows the energy band diagrams corresponding to sample D showing that the effective barrier height in this case was similar to that for ternary AlGaIn.

We designed a second non-random alloy barrier based on a polarization-engineered binary GaN barrier (sample B1) (Figure 3(b)). As shown in the energy band diagram (Figure 3(c)), a thin InGaIn²⁰ layer provides a polarization-induced dipole that creates an electrostatic barrier that would not be permeable to percolation effects. The InGaIn layer was grown in In-rich conditions using a Ga/N flux ratio of 0.40 at a temperature of 540 °C.^{20–23} In the energy band diagram simulation, background density of 10^{16} cm^{-3} n-type dopants for GaN layer was included. The AlGaIn layer was used to further provide a dipole at the UID GaN/AlGaIn interface, which leads to a flat energy band profile at equilibrium.

Figures 3(d) and 3(e) show the vertical I–V characteristics in linear and log-scales, respectively, of the random alloy barrier (R), the digital alloy barrier (D1), and the polarization engineered electrostatic barrier (B1). The samples with non-random digital (D1) and electrostatic binary GaN (B1) barriers had more than 3 orders of magnitude lower leakage current density than the sample R (random alloy) for reverse bias in the range of <2 V, even though the effective barrier height from the energy band diagram in these cases is nominally the same. The low reverse bias leakage characteristic is not top-contact limited since the

lateral current between two top-contact pads of a device exhibits linear Ohmic behavior (inset to Figure 3(d)). This significant reduction in vertical leakage using a polarization-engineered electrostatic and a digital alloy ($\text{Al}_{0.3}\text{Ga}_{0.7}\text{N}$) as barriers confirms our hypothesis that eliminating a ternary random alloy as the barrier does prevent percolation-based transport of electrons.

The results presented here are of great significance to vertical unipolar III-nitride devices since excess leakage in such structures had prevented them from achieving their theoretical performance. In addition, our work is also significant in understanding forward and reverse bias gate characteristics for III-Nitride AlGaIn/GaN HEMTs and metal-insulator transistor HEMTs, and electron barrier layers in III-nitride LEDs. In the case of MISHEMTs, forward bias on the gate has been found to create a large electron accumulation at the insulator/oxide interface even at low effective forward voltage, where tunneling through the AlGaIn should be minimal. Our work on understanding and eliminating percolation transport through the barrier could help to eliminate these effects and enable normally off power transistors that operate at positive gate bias.

In conclusion, we investigated unipolar transport in GaN/AlGaIn/GaN heterostructures and found the reverse bias leakage to be independent of TDDs as well as of heterojunction potential heights. It is hypothesized that random alloy fluctuations in the ternary AlGaIn barrier lead to percolation-based transport which enables electrons to flow through the ternary barrier. This hypothesis is supported by simulations performed using a 2D FEM drift-diffusion transport model incorporating statistical fluctuations of Al-compositions in the AlGaIn barrier. It was further tested experimentally by reducing the vertical leakage by more than 3 orders of magnitude by using non-random alloy based barriers based on digital $\text{Al}_{0.3}\text{Ga}_{0.7}\text{N}$ and polarization-engineered binary GaN barriers. This understanding of unipolar transport characteristics and means of reducing the

vertical leakage in GaN/AlGaIn/GaN heterostructures hold promise for a variety of unipolar III-nitride devices, and for other devices such as HEMTs and LEDs that use random AlGaIn alloy-based electron blocking layers.

This work was funded by the Office of Naval Research (ONR N00014-11-1-0721 [Dr. Paul Maki] under DATE MURI). The modeling work was partially supported by National Science Council in Taiwan by Grant Nos. 99-2221-E-002-058-MY3. The authors would like to thank Dr. Aaron Arehart for low temperature measurements.

- ¹C. Bayram, Z. Vashaei, and M. Razeghi, *Appl. Phys. Lett.* **96**, 042103-3 (2010).
- ²M. Hermann, E. Monroy, A. Helman, B. Baur, M. Albrecht, B. Daudin, O. Ambacher, M. Stutzmann, and M. Eickhoff, *Phys. Status Solidi C* **1**, 2210–2227 (2004).
- ³S. Leconte, F. Guillot, E. Sarigiannidou, and E. Monroy, *Semicond. Sci. Technol.* **22**, 107–112 (2007).
- ⁴A. F. J. Levi and T. H. Chiu, *Appl. Phys. Lett.* **51**, 984–986 (1987).
- ⁵S. Dasgupta, A. Raman, J. S. Speck, and U. K. Mishra, *IEEE Electron Device Lett.* **32**, 1212–1214 (2011).
- ⁶M. Heiblum, I. M. Anderson, and C. M. Knoedler, *Appl. Phys. Lett.* **49**, 207–209 (1986).
- ⁷U. K. Reddy, J. Chen, C. K. Peng, and H. Morkoc, *Appl. Phys. Lett.* **48**, 1799–1801 (1986).
- ⁸M. Heiblum, D. C. Thomas, C. M. Knoedler, and M. I. Nathan, *Appl. Phys. Lett.* **47**, 1105–1107 (1985).
- ⁹I. Ben-Yaacov, Y.-K. Seck, U. K. Mishra, and S. P. DenBaars, *J. Appl. Phys.* **95**, 2073–2078 (2004).
- ¹⁰S. Chowdhuri, M. H. Wong, B. L. Swenson, and U. K. Mishra, *IEEE Electron Device Lett.* **33**, 41–43 (2012).
- ¹¹See supplementary material at <http://dx.doi.org/10.1063/1.4813309> for reference to BANDENG, Atlas Silvaco, Ammono, St. Gobain and figures for dislocation-mediated leakage.
- ¹²S. Karmalkar, D. M. Sathaiya, and M. S. Shur, *Appl. Phys. Lett.* **82**, 3976–3978 (2003).
- ¹³D. Li, L. Tang, C. Edmunds, J. Shao, G. Gardner, M. J. Manfra, and O. Malis, *Appl. Phys. Lett.* **100**, 252105-4 (2012).
- ¹⁴P. J. W. Hsu, M. J. Manfra, R. J. Molnar, B. Heying, and J. S. Speck, *Appl. Phys. Lett.* **81**, 79–81 (2002).
- ¹⁵S. Kaun, M. H. Wong, S. Dasgupta, S. Choi, R. Chung, U. K. Mishra, and J. S. Speck, *Appl. Phys. Exp.* **4**, 024101-3 (2011).
- ¹⁶D. S. Li, H. Chen, H. B. Yu, H. Q. Jia, Q. Huang, and J. M. Zhou, *J. Appl. Phys.* **96**, 1111–1114 (2004).
- ¹⁷M. F. Schubert, S. Chhajed, J. K. Kim, E. F. Schubert, D. D. Koleske, M. H. Crawford, S. R. Lee, and A. J. Fischer, *Appl. Phys. Lett.* **91**, 231114-3 (2007).
- ¹⁸Y.-R. Wu, R. Shivaraman, K.-C. Wang, and J. S. Speck, *Appl. Phys. Lett.* **101**, 083505-4 (2012).
- ¹⁹C.-K. Li and Y.-R. Wu, *IEEE Trans. Electron. Device* **59**, 400–407 (2012).
- ²⁰D. Nath, E. Gur, S. A. Ringel, and S. Rajan, *J. Vac. Sci. Technol. B* **29**, 021206-7 (2011).
- ²¹F. Akyol, D. N. Nath, E. Gur, P. S. Park, and S. Rajan, *Jpn. J. Appl. Phys., Part 1* **50**, 052101-3 (2011).
- ²²S. Krishnamoorthy, D. N. Nath, F. Akyol, P. S. Park, M. Esposto, and S. Rajan, *Appl. Phys. Lett.* **97**, 203502-3 (2010).
- ²³S. Krishnamoorthy, P. S. Park, and S. Rajan, *Appl. Phys. Lett.* **99**, 233504-3 (2011).